Research Paper

TMEM126B deficiency reduces mitochondrial SDH oxidation by LPS, attenuating HIF-1α stabilization and IL-1β expression

Dominik C. Fuhrmann[a], Ilka Wittig[b], Bernhard Brüne[a],*

[a] *Institute of Biochemistry I, Faculty of Medicine, Goethe-University Frankfurt, Germany*
[b] *Functional Proteomics, SFB 815 Core Unit, Goethe-University Frankfurt, Germany*

ABSTRACT

Mitochondrial derived reactive oxygen species (mtROS) are known for their signaling qualities in both physiology and pathology. To elucidate mitochondrial complex I-dependent ROS-signaling after lipopolysaccharide (LPS)-stimulation THP-1 macrophages with a knockdown of the transmembrane protein TMEM126B were generated. TMEM knockdown cells (sh126B) showed a reduced assembly of complex I and attenuated mtROS production. In these cells we identified protein oxidization by mtROS upon LPS-treatment using the BIAM switch assay coupled to liquid chromatography and mass spectrometry. One of the identified targets of mtROS was succinate dehydrogenase (SDH) flavoprotein subunit A (SDHA). Oxidation of SDHA decreased its enzymatic activity and pharmacological inhibition of SDH in turn stabilized hypoxia inducible factor (HIF)-1α and caused the subsequent, sustained expression of interleukin-1β (IL-1β). Oxidation of SDHA in sh126B cells was attenuated, while pharmacological inhibition of SDH by atpenin A5 restored IL-1β expression in sh126B cells upon LPS-treatment. Conclusively, oxidation of SDH by mtROS links an altered metabolism, i.e. succinate accumulation to HIF-1-driven, inflammatory changes in macrophages.

1. Introduction

Transmembrane protein 126B (TMEM126B) is a complex I assembly factor. Together with acyl-CoA dehydrogenase family member 9, evolutionary conserved signaling intermediate in toll pathway (ECSIT), and complex I intermediate-associated protein 30 TMEM126B forms the mitochondrial complex I assembly complex [1,2]. This assembly complex in combination with the translocase of inner mitochondrial membrane domain containing protein facilitates gathering and incorporation of the Q-module into complex I of the mitochondrial respiratory chain [3]. Thereby, TMEM126B adds to the correct functional composition of the 45 subunits containing complex I [4,5]. Defects in TMEM126B are associated with complex I deficiencies and a decreased cellular respiratory capacity [6,7]. This was substantiated under chronic hypoxia, which provoked TMEM126B degradation and partial inactivation of complex I [8].

Mitochondria are known as a potential source of reactive oxygen species (ROS) [9]. Particularly, complex I and III, but also complex II (further referred to as succinate dehydrogenase, SDH) produce ROS [10]. Spatial analysis revealed that complex I and SDH release ROS into the matrix, while complex III ROS spills predominantly into the intermembrane space, thereby generating very distinct oxidation patterns

[11]. Mitochondrial ROS are important mediators in toll like receptor 4 (TLR4) signaling, inflammasome activation, and thus cytokine production [12]. Interestingly, ECSIT is needed to generate mtROS and cytokine signaling after TLR4-stimulation, a pathway interrupted by peroxiredoxin 6 [13,14]. In the context of inflammatory cytokine formation, the hypoxia inducible factor (HIF)-1α also gained some interest. HIF-1α coordinates metabolism and proinflammatory cytokine production in classically activated macrophages [15]. Specifically, interleukin (IL)-1β, IL-10, and IL-11 production is HIF-1-dependent [16–18]. Among these cytokines, IL-1β initiates a positive feedback loop to induce HIF-1α, possibly via NF-κB activation [19]. HIF consists of an alpha (HIF-1α, HIF-2α) and corresponding beta (HIF-1β) subunit. Under ambient oxygen concentrations, the HIFα subunit is continuously degraded by prolyl hydroxylases (PHDs) [20]. When oxygen is lacking, PHDs are inhibited, HIF-1α translocates to the nucleus, dimerizes with HIF-1β, and facilitates target gene expression. Besides hypoxia other factors such as mitochondrial ROS (mtROS) or distinct tricarboxylic acid (TCA) cycle intermediates, e.g. succinate may stabilize HIF-1α even under normoxic conditions [21–23]. Under inflammatory conditions succinate accumulation creates a state of pseudohypoxia because of HIF-1α stabilization, which in turn sustains an inflammatory macrophage phenotype. So far stabilization of HIF-1α

was linked to complex III ROS under hypoxia but also non mitochondrial sources such as NADPH oxidases are discussed [24–26]. However, the induction of HIF-1α by mtROS is highly debated as in cells lacking mitochondrial DNA mtROS are dispensable for oxygen-dependent HIF-1α stabilization [27–29]. Also, mechanisms how ROS affect HIF under normoxia are not fully explored. This study provides evidence that formation of mtROS in LPS-stimulated macrophages causes oxidation and inactivation of SDH. In turn, HIF-1α gets stabilized and sustains IL-1β expression.

2. Material and methods

2.1. Cell culture

THP-1 cells (derived from a male donor) were incubated at 37 °C with 5% CO_2 in DMEM medium (GE Healthcare, Munich, Germany) with 10% FCS and 1% penicillin/streptomycin (PAA Laboratories, Cölbe, Germany). THP-1 cells were stably transduced with a lentiviral shRNA (Mission shRNA) against TMEM126B (sh126B: V2LHS_175840) and selected using puromycin. Controls (shC) are THP-1 cells transduced with a pLKO.1-puro vector.

2.2. Treatments

If not indicated differently, cells were treated with 1 μg/ml lipopolysaccharide (LPS, Sigma-Aldrich, Munich, Germany), 1 μM atpenin A5 (AA5, Cayman Chemicals, Michigan, USA), 100 μM mitoTEMPO (TEMPO, Sigma-Aldrich), 20 mM dimethyl succinate (DMS, Sigma-Aldrich), or 50 nM rotenone (Rot, Sigma-Aldrich).

2.3. Western analysis

Cells were lysed in a buffer containing 4% SDS, 150 mM NaCl, and 100 mM Tris/HCl, pH 7.4, and sonicated. Protein content was determined by a protein assay kit (Bio-Rad, Munich, Germany) and 100 μg protein were loaded on a 10% SDS gel. Gels were blotted using a Trans Blot Turbo blotting system (Bio-Rad). Membranes were blocked in 5% milk in TBS-T for IL-1β (Cell signaling technology, Frankfurt, Germany), HIF-1α (Novus Biologicals, Wiesbaden, Germany), nucleolin (Santa Cruz, Heidelberg, Germany), and tubulin (Sigma-Aldrich), or 5% BSA in TBS-T for TMEM126B (Atlas Antibodies via Sigma) and SDHA (Atlas Antibodies via Sigma-Aldrich). Enhanced chemiluminescence on a C-DIGIT scanner (Licor, Lincoln, USA) or fluorescence on an Odyssey scanner (Licor) was quantified with Image Studio Digits 5.0 (Licor).

2.4. Real time PCR

RNA was isolated using peqGold (Peqlab, Erlangen, Germany) and measured using a Nanodrop ND-1000 spectrophotometer (Peqlab). Reverse transcription was performed with the Maxima First Strand cDNA Synthesis Kit for RT-PCR (Thermo Fisher Scientific, Waltham, USA). RNA expression of TMEM126B (fwd: 5'-GGTGGTGTTCGGGTATGAGG-3', rev: 5'-TCTTGAAAACCTTGGGCGCT-3'), Glut1 (fwd: 5'-TCACTGTGCTCCTGGTTCTG-3', rev: 5'-CCTGTGCTCCTGAGAGATCC-3'), IL-1β (fwd: 5'-TCTTTAACGCAGGACAG-3', rev: 5'-TTCGACACATGGGATAACGA-3'), and HIF-1α (fwd: 5'-GCTGGCCCCAGCCGCTGGAG-3', rev: 5'-GAGTGCAGGGTCAGCACTAC-3') was analyzed using SYBR green fluorescent mix (Thermo Fischer Scientific) on a CFX96 Real Time PCR Detection System (Bio-Rad) and normalized to TBP (fwd: 5'-GGGCCGCCGGCTGTTTAACT-3', rev:5'-GGGCCGCCGGCTGTTTAACT-3'). BNIP3 primers were purchased from Quiagen (Hilden, Germany).

2.5. Flow cytometry

THP-1 cells were stained with MitoTracker Green (200 nM, Thermo Fischer Scientific) or MitoSox (5 μM, Thermo Fischer Scientific) for 20 min, washed with PBS and resuspended in FACS-Flow before measurement. Cytometric bead arrays (CBA) were performed using a BD CBA Flex Set for IL-1β (BD, Heidelberg, Germany). Supernatants were incubated for 1 h with the antibody. Afterwards, beads were added, incubated for 2 h, washed, and measured by FACS.

2.6. Seahorse

The cellular oxygen consumption rate (OCR) and the extracellular acidification rate (ECAR) were analyzed using a Seahorse 96 extracellular flux analyzer (Agilent, Santa Clara, USA). THP-1 cells were plated in Seahorse 96-well cell culture plates at 50.000 cells/well at the day of measurement and equilibrated for 1 h before measurement in Krebs Henseleit buffer (111 mM NaCl, 4.7 mM KCl, 1.25 mM $CaCl_2$, 2 mM $MgSO_4$, 1.2 mM Na_2HPO_4) supplemented with 25 mM L-glucose and 3 mM L-glutamine. Cells were treated with 2.5 μM oligomycin (Sigma-Aldrich) to block ATP-coupled respiration, 1 μM carbonyl cyanide m-chlorophenylhydrazone (CCCP) (Sigma-Aldrich) to uncouple the respiratory chain, and 1 μg/ml antimycin A (Sigma-Aldrich) together with 1 μM rotenone (Sigma-Aldrich) to block mitochondrial respiration.

2.7. Metabolic assays

The NAD/NADH assay (abcam, Cambridge, UK), ATP assay (BioVision, Milpitas, USA), and SDH activity assay (BioVision) were performed according to manufacturer's guidelines.

2.8. BIAM switch assay

Proteins were precipitated in 20% trichloroacetic acid (TCA) by centrifugation for 30 min at $16.000 \times g$ and washed with 10% TCA and 5% TCA, respectively. Pellets were resuspended in 200 μl NEM-DAB (8 M Urea, 5 mM EDTA, 0.5% SDS, 50 mM Tris/HCL, pH 8.5, 50x molar of estimated cysteine thiols NEM) and incubated at 850 rpm for 1 h at 22 °C in the dark. Proteins were precipitated by ice-cold acetone, collected by centrifugation, washed, resuspended in 150 μl DTT-DAB (8 M Urea, 5 mM EDTA, 0.5% SDS, 50 mM Tris/HCL, pH 8.5, 3 mM DTT) and incubated at 850 rpm for 5 min at 22 °C in the dark followed by addition of 150 μl BIAM-DAB (8 M Urea, 5 mM EDTA, 0.5% SDS, 50 mM Tris/HCL, pH 8.5, 50x molar of estimated cysteine thiols BIAM) and incubated at 850 rpm for 1 h at 22 °C in the dark. Proteins were precipitated with ice-cold acetone overnight at −20 °C, collected by centrifugation, washed, and resuspended in 100 μl lysis buffer (5 mM EDTA, 50 mM Tris/HCL pH 8.5, 1% Triton-X-100, 1% SDS). 350 μg of proteins were affinity purified using agarose streptavidin beads overnight at 4 °C on a wheel. After washing, beads were resuspended in 50 μl 6 M GdmCl, 50 mM Tris/HCl, pH 8.5 and incubated at 95 °C for 5 min. Samples were diluted with 25 mM Tris/HCl, pH 8.5, 10% acetonitrile to obtain a final GdmCl concentration of 0.6 M.

2.9. BIAM switch mass spectrometry

Proteins were digested with 1 μg trypsin (sequencing grade, Promega) overnight at 37 °C under gentle agitation. Digestion was stopped by adding trifluoroacetic acid to a final concentration of 0.5%. Peptides were loaded on multi-stop-and-go tip (StageTip) containing six C18 discs. Purification and elution of peptides was performed as described in [30]. Peptides were eluted in wells of microtiter plates and peptides were dried and resolved in 1% acetonitrile, 0.1% formic acid. Liquid chromatography/mass spectrometry (LC/MS) was performed on Thermo Scientific™ Q Exactive Plus equipped with an ultra-high performance liquid chromatography unit (Thermo Scientific Dionex Ultimate 3000) and a Nanospray Flex Ion-Source (Thermo Scientific). Peptides were loaded on a C18 reversed-phase precolumn (Thermo Scientific) followed by separation on 2.4 μm Reprosil C18 resin (Dr.
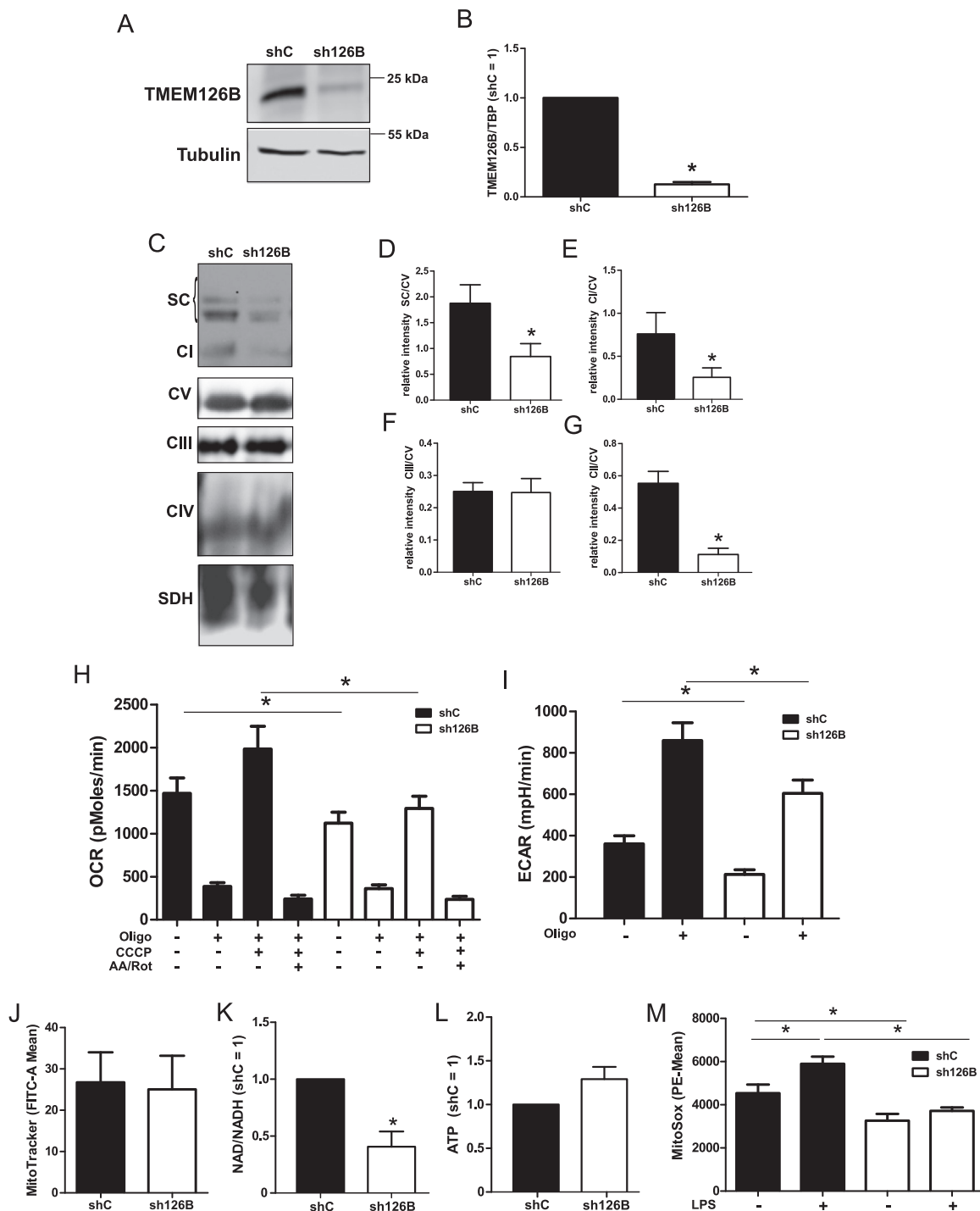
Fig. 1. Characterization of TMEM126B knockdown cells. A. Western analysis of transmembrane protein 126B (TMEM126B) and tubulin in control cells (shC) and TMEM126B knockdown cells (sh126B). B. mRNA analysis of TMEM126B in shC (black bars) and sh126B cells (white bars). C. Blue native electrophoresis coupled with Western analysis for NADH-dehydrogenase [ubiquinone] 1 beta subcomplex subunit 8 (NDUFB8) of complex I (CI) and supercomplexes (SC), ATP synthase subunit alpha (ATP5A) of complex V (CV), cytochrome b-c1 complex subunit 2 (UQCRC2) of complex III (CIII), cytochrome c oxidase subunit 2 (Cox2) of complex IV (CIV), and succinate dehydrogenase [ubiquinone] iron-sulfur subunit (SDHB) of complex II (CII). D-G. Quantification of blue native electrophoresis for SC (D), CI (E), CIII (F), and CII (G) normalized to CV (n = 4). H. Oxygen consumption rate (OCR) in shC and sh126B cells sequentially treated with oligomycin (2.5 μM, Oligo), carbonyl cyanide m-chlorophenylhydrazone (1 μM, CCCP), and antimycin A (1 μg/ml AA) together with rotenone (1 μM, Rot) (n = 3). I. Extracellular acidification rate (ECAR) in shC and sh126B cells treated with oligomycin (2.5 μM, Oligo) (n = 3). J. Flow cytometric analysis of mitoTracker Green stained shC and sh126B cells (n = 3). K. Determination of the NAD/NADH ratio in shC and sh126B cells (n = 12). L. Relative ATP amount measurement in shC and sh126B cells (n = 7). M. Flow cytometric analysis of mitoSox stained shC and sh126B cells treated 4 h with LPS (n = 11). All data are mean values ± SEM, *p < 0.05.

Maisch GmbH, Ammerbuch-Entringen, Germany) in-house packed pi-cotip emitter tip (diameter 100 μm, 15 cm long from New Objectives) using a gradient from mobile phase A (4% acetonitrile, 0.1% formic acid) to 30% mobile phase B (99% acetonitrile, 0.1% formic acid) for

90 min followed by a second gradient to 60% B for 15 min with a flow rate 350 nl/min. MS data were recorded by data dependent acquisition Top10 method selecting the most abundant precursor ions in positive mode for HCD fragmentation. Lock mass option was enabled to ensure

high mass accuracy between multiple runs [31]. The Full MS scan range was 300–2000 m/z with resolution of 70,000, and an automatic gain control (AGC) value of $3*10^6$ total ion counts with a maximal ion injection time of 160 ms. Only higher charged ions (2 +) were selected for MS/MS scans with a resolution of 17500, an isolation window of 2 m/z and an automatic gain control value set to 10^5 ions with a maximal ion injection time of 150 ms. Selected ions were excluded in a time frame of 30 s following fragmentation event. Fullscan data were acquired in profile and fragments in centroid mode by Xcalibur software.

2.10. Data analysis of MS data

For data analysis MaxQuant 1.6.1.0, Perseus 1.5.6.0, and Excel (Microsoft Office 2013) were used [32,33]. N-terminal acetylation (+ 42.01) and oxidation of methionine (+ 15.99), N-ethylameimide on cysteines (+ 125.05) and biotinylated iodoacetamide (+ 414.19) were selected as variable modifications. The human reference proteome set (Uniprot, July 2017, 701567 entries) was used to identify peptides and proteins with a false discovery rate (FDR) less than 1%. Minimal ratio count for label-free quantification (LFQ) was 1. Reverse identifications and common contaminants were removed and the data-set was reduced to proteins that were identified in at least 4 of 6 samples in one experimental group. Missing values were replaced from normal distribution and two sample t-test was performed considering p < 0.05 as significant. To visualize significantly oxidized proteins, scatter plots were created, which visualize changes in oxidation by potting log t-test p-values (proteins above the horizontal line are considered as significant) against the difference of the compared conditions (vertical line separates conditions).

2.11. Isolation of mitochondria

THP-1 cells were washed, harvested in PBS, centrifuged (10 min, 1.000 × g, 4 °C), and resuspended in CCM I buffer (250 mM sucrose, 1 mM EDTA, 20 mM Tris/HCl, pH 7.4) containing protease-inhibitor (Roche, Grenzach-Wyhlen, Germany). The suspension was pressed ten times through a 25 G needle, followed by centrifugation (10 min, 1.000 × g, 4 °C). The supernatant was centrifuged again (10 min, 6.000 × g, 4 °C) and the resulting pellet was resuspended in CCM I. Protein content was measured by Lowry (Bio Rad).

2.12. Isolation of macromolecular complexes by blue native gels

Isolated mitochondria were aliquoted into portions of 400 μg protein and sedimented to obtain pellets. Mitochondria were resuspended in 40 μl buffer A (50 mM NaCl, 50 mM imidazole pH 7, 1 mM EDTA, 2 mM aminocaproic acid) and solubilized with 16 μl 20% digitonin (w/v in water) to obtain a detergent/protein ratio of 8 g/g. Samples were centrifuged for 10 min at 22.000 × g and protein content of the supernatant was determined. 50 μg total protein was loaded onto gradient (3–16%) gels followed by blue native electrophoresis (BNE) [34].

2.13. Statistics

Data are expressed as mean values ± SEM. Statistically significant differences were calculated after analysis of variance (ANOVA) and Bonferroni's test or Students t-test; p < 0.05 was considered significant.

3. Results and discussion

3.1. Characterization of a TMEM126B knockdown in THP-1 cells

Considering degradation of TMEM126B under chronic hypoxia we became interested to study the function of this complex I assembly factor in THP-1 cells [8]. A knockdown of TMEM126B was generated by

transducing monocytic THP-1 cells with shRNA against TMEM126B (sh126B), while a non-targeted shRNA (shC) served as a control. Knockdown efficacy was validated at protein and mRNA level (Fig. 1 A and B). Taking into account that TMEM126B helps to assemble complex I, we analyzed the respiratory chain composition by blue native gel electrophoresis using isolated mitochondria.

Expression of NADH-dehydrogenase [ubiquinone] 1 beta subcomplex subunit 8 (NDUFB8), a measure for complex I, decreased in sh126B cells (Fig. 1C). In addition, supercomplex formation was impaired (Fig. 1C and D). In contrast, complex III (cytochrome b-c1 complex subunit 2, UQCRC2), IV (cytochrome c oxidase subunit 2), and V (ATP synthase subunit alpha) remained unaltered. The amount of SDH (complex II), followed by the expression of succinate dehydrogenase [ubiquinone] iron-sulfur subunit B, was lowered in sh126B compared to control cells (Fig. 1C to 1G). We then followed oxygen consumption rates (OCR) of shC and sh126B cells by a Seahorse XFe 96 flux analyzer (Fig. 1H, S1). Basal respiration was higher in shC compared to sh126B cells. Oligomycin (Oligo) reduced OCR of both clones to the same extent, while uncoupling the electron transport chain by carbonyl cyanide m-chlorophenylhydrazone (CCCP) provoked its increase. CCCP increased oxygen consumption rates in shC above basal levels, which was not the case in sh126B cells. Inhibition of complex I and III by rotenone (Rot) and antimycin A (AA) decreased OCR to values seen with oligomycin, both in shC and sh126B cells. A reduction in OCR in sh126B cells goes along with a lower amount of functional complex I. Subsequent experiments captured extracellular acidification (ECAR), an indication of the glycolytic activity. Unexpectedly, sh126B cells revealed a lower ECAR compared to shC, while the addition of oligomycin enhanced ECAR in both clones (Fig. 1I). Reduced levels of ECAR in sh126B pointed to a reduced glycolytic capacity. To exclude that an altered number of mitochondria account for these differences, we used MitoTracker green and FACS analysis to prove an equivalent mitochondrial mass in shC and sh126B cells (Fig. 1J). To substantiate a functional role of the TMEM126B knockout towards complex I, we assessed the NAD/NADH ratio (Fig. 1K). The lower NAD/NADH ratio in sh126B compared to shC cells indicates accumulation of the complex I substrate NADH. This coincides with reduced complex I abundance in sh126B cells. We then measured ATP levels in shC and sh126B cells and noticed no difference (Fig. 1L). This strongly argues for the use of alternative energy sources such as glutamine. Glutamine can be processed to α-ketoglutarate and metabolized to succinate, to fuel the TCA-cycle, and consequently provides electrons for oxidative phosphorylation [35]. This pathway may increase ATP-production via TCA-cycle products and would explain reduced glycolysis in sh126B cells [36]. Although the TMEM126B knockdown decreases complex I abundance and consequently its activity, the resting respiratory capacity was lowered but not completely repressed. Apparently, the remaining components of the respiratory chain (complex III-IV) are functional and consume oxygen. To consume oxygen, electrons must be fed into the electron transporting chain. Thus, SDH may provide electrons from succinate to ubiquinone [37]. Alternatively, electrons can either be provided by acyl-CoA dehydrogenases and electron transfer flavoproteins, or by glycerol-3-phosphate dehydrogenase [38]. In either case, electrons are transferred from ubiquinone to complex III and IV to reduce molecular oxygen and thus, explain residual oxygen consumption despite complex I inhibition.

3.2. mtROS production is impaired in sh126B

A functionally impaired complex I in sh126B cells provoked the question whether the redox state of these cells might be affected. Therefore, we measured mtROS production using MitoSOX in combination with flow cytometry (see Fig. S2A and S2B for time-dependencies and DHE-staining). As mtROS are intimately linked to TLR4 signaling, we analyzed mtROS production upon LPS-treatment in wild type or sh126B THP-1 cells (Fig. 1M). Basal mtROS levels were
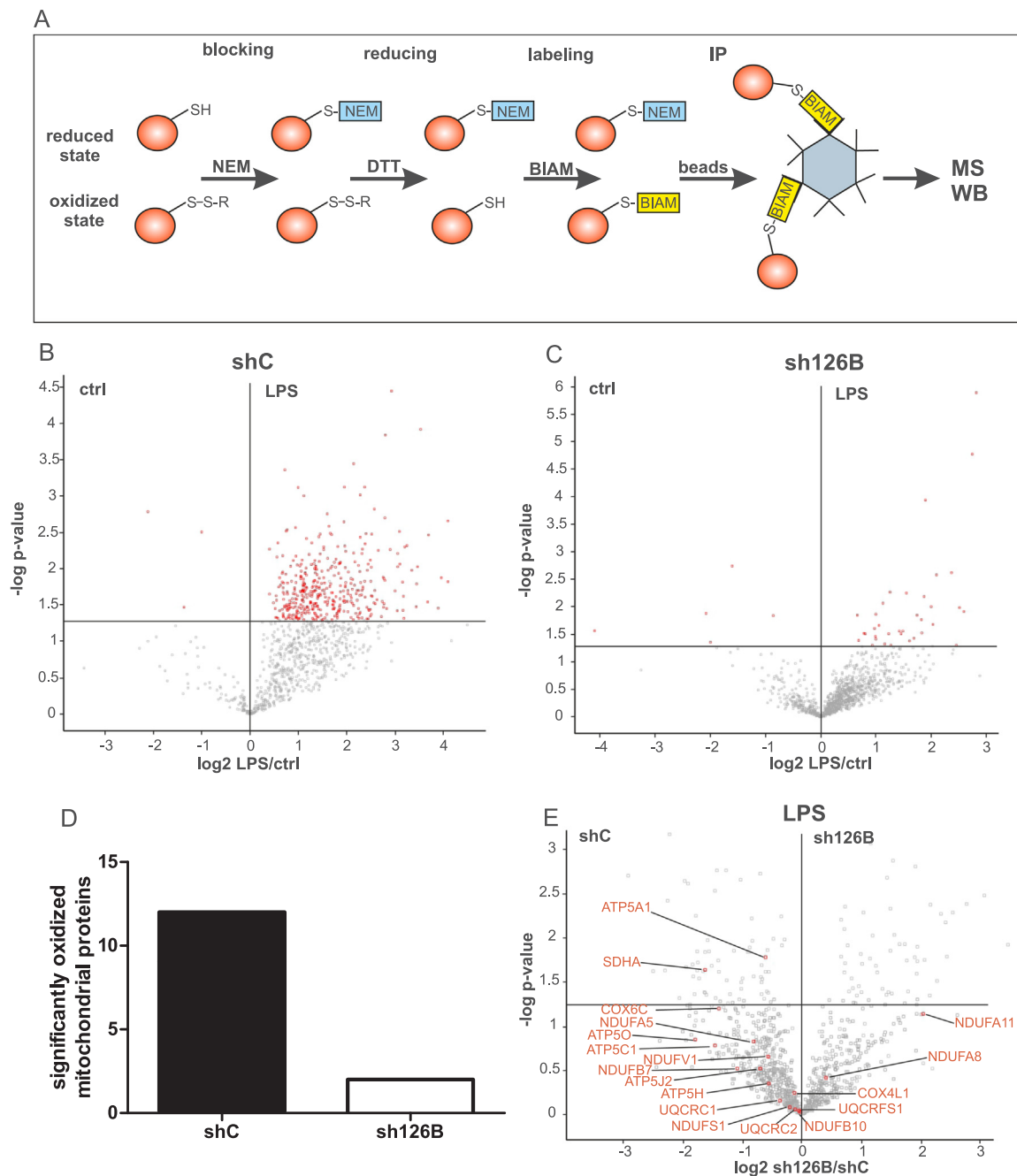
Fig. 2. BIAM switch assay. A. Workflow of the EZ-Link Iodoacetyl-PEG2-Biotin (BIAM) switch assay. B. Analysis of untreated (ctrl) and 4 h LPS-treated control cells (shC) (n = 6). Red dots indicate significantly oxidized protein after LPS-treatment. C. Analysis of untreated (ctrl) and LPS-treated TMEM126B knockdown cells (sh126B) (n = 6). Red dots indicate significantly oxidized protein after LPS-treatment. D. After LPS treatment the number of significantly oxidized mitochondrial proteins in shC and sh126B was depicted as bar graph. E. Proteins involved in oxidative phosphorylation were analyzed in LPS-treated shC compared to sh126B cells (n = 6). Red dots indicate proteins of the respiratory chain. Students *t*-test values p < 0.05 were considered as significant.

significantly reduced in sh126B cells, likely due to a compromised complex I activity. Following TLR4-activation by LPS, mtROS increased in shC but not in sh126B cells. Conclusively, basal as well as LPS-stimulated mtROS production is attenuated as a consequence of the TMEM126B knockdown. Along these redox changes, we stained oxidized proteins in isolated mitochondria using IRDye 800 maleimide and fluorescence detection (Fig. S2C and S2D). In LPS-stimulated shC cells oxidation of mitochondrial proteins increased from 2 to 4 h. This only occurred at a drastically lower rate in sh126B cells.

Often complex I inactivation or inhibition goes in line with increased ROS production. Complex I inhibitors such as the antiviral drug efavirenz or the Q-site inhibitor rotenone promote ROS production at

complex I [39,40]. In contrast, the TMEM126B knockdown decreases mtROS production, making our model a promising tool to study effects of mtROS on protein oxidation after LPS-treatment and TLR4-signaling.

3.3. LPS-mediated oxidations are reduced in sh126B

To gain more detailed information on LPS-induced ROS formation linked to protein oxidation, we performed a BIAM switch assay coupled to mass spectrometry (MS) (Fig. 2A). To identify oxidized proteins, free cysteine thiols are blocked with NEM. Afterwards, oxidized cysteines are reduced by DTT, subsequently labeled with BIAM for immunoprecipitation, followed by quantitative mass spectrometry.

Table 1

Significantly oxidized proteins in shC compared to sh126B cells after LPS treatment arranged by descendant significance (mitochondrial proteins are highlighted in yellow).

significantly oxidized only in shC	
Protein names	**Gene names**
Aldo-keto reductase family 1 member C2	AKR1C2
Peptidyl-prolyl cis-trans isomerase F, mitochondrial	PPIF
Aldo-keto reductase family 1 member C3	AKR1C3
Heterogeneous nuclear ribonucleoprotein H3	HNRNPH3
Programmed cell death protein 4	PDCD4
Cyclin-dependent kinase 1	CDC2;CDK1
Myosin regulatory light chain 12A;Myosin regulatory light chain 12B	MYL12A;MYL12B
Glutamate dehydrogenase 1, mitochondrial	GLUD1
NAD(P) transhydrogenase, mitochondrial	NNT
Dynactin subunit 2	DCTN2
Serine/threonine-protein phosphatase 2A catalytic subunit alpha isoform	PPP2CA
G-rich sequence factor 1	GRSF1
D-3-phosphoglycerate dehydrogenase	PHGDH
Glutaredoxin-3	GLRX3
Enoyl-CoA hydratase, mitochondrial	ECHS1
Sideroflexin;Sideroflexin-3	SFXN3
RNA-binding motif protein	RBMX
DNA-directed RNA polymerases I, II, and III subunit RPABC3	POLR2H
3-hydroxyisobutyrate dehydrogenase, mitochondrial	HIBADH
Complement component 1 Q subcomponent-binding protein, mitochondrial	C1QBP
Calcium-binding and coiled-coil domain-containing protein 2	CALCOCO2
Thioredoxin-dependent peroxide reductase, mitochondrial	PRDX3
U2 small nuclear ribonucleoprotein A	SNRPA1
Small nuclear ribonucleoprotein G	SNRPG
Succinate dehydrogenase [ubiquinone] flavoprotein subunit, mitochondrial	SDHA
Programmed cell death 6-interacting protein	PDCD6IP
Gelsolin	GSN
Transformer-2 protein homolog beta	TRA2B
Serine/threonine-protein phosphatase 6 catalytic subunit	PPP6C
Protein DEK	DEK
Heat shock protein 105 kDa	HSPH1
Sorting nexin-5	SNX5
SUMO-activating enzyme subunit 1;SUMO-activating enzyme subunit 1, N-terminally processed	SAE1
Acyl-coenzyme A thioesterase 1;Acyl-coenzyme A thioesterase 2, mitochondrial	ACOT1;ACOT2
26S protease regulatory subunit 8	PSMC5
Phosphoglycerate mutase 1	PGAM1
Rab GDP dissociation inhibitor beta	GDI2
ATP-dependent RNA helicase DDX3X	DDX3X
Exportin-2	CSE1L
Voltage-dependent anion-selective channel protein 2	VDAC2
Coiled-coil domain-containing protein 47	CCDC47
Thioredoxin-like protein 1	TXNL1
Protein Red	IK
40S ribosomal protein S16	RPS16
Guanine nucleotide-binding protein G(i) subunit alpha-2	GNAI2
Nuclear autoantigenic sperm protein	NASP
Tubulin beta-6 chain	TUBB6
Ras GTPase-activating protein-binding protein 1	G3BP1
60S ribosomal protein L38	RPL38
Polyadenylate-binding protein 1;Polyadenylate-binding protein	PABPC1
6-phosphogluconate dehydrogenase, decarboxylating	PGD
Clathrin heavy chain;Clathrin heavy chain 1	CLTC
ADP/ATP translocase 2;ADP/ATP translocase 2, N-terminally processed	SLC25A5
ATP synthase subunit alpha, mitochondrial	ATP5A1
Trifunctional purine biosynthetic protein adenosine-3	GART
RNA-binding protein 42	RBM42
Rho GDP-dissociation inhibitor 1	ARHGDIA
Nucleophosmin	NPM1
40S ribosomal protein S9	RPS9
tRNA pseudouridine synthase;tRNA pseudouridine synthase A, mitochondrial	PUS1
V-type proton ATPase subunit E 1	ATP6V1E1
ATP synthase subunit beta, mitochondrial;ATP synthase subunit beta	ATP5B
40S ribosomal protein SA	RPSA
Histone H1.3	HIST1H1D
60S ribosomal protein L18	RPL18

(continued on next page)

Table 1 (*continued*)

significantly oxidized only in sh126B	
Protein names	**Gene names**
Aminopeptidase N	ANPEP
Laminin subunit gamma-1	LAMC1
Annexin A4	ANXA4
Procollagen-lysine,2-oxoglutarate 5-dioxygenase 1	PLOD1
Twisted gastrulation protein homolog 1	TWSG1
Azurocidin	AZU1
Annexin A1;Annexin	ANXA1
CD166 antigen	ALCAM
Integrin alpha-L	ITGAL
Bone morphogenetic protein 8B;Bone morphogenetic protein 8A	BMP8B;BMP8A
Thioredoxin	TXN
Procollagen galactosyltransferase 1	COLGALT1
DnaJ homolog subfamily C member 10	DNAJC10
Adipocyte plasma membrane-associated protein	APMAP
Leukocyte immunoglobulin-like receptor subfamily B member 4	LILRB4
Splicing factor 1	SF1
Ferritin light chain	FTL
Cartilage-associated protein	CRTAP
Procollagen-lysine,2-oxoglutarate 5-dioxygenase 3	PLOD3
IgG receptor FcRn large subunit p51	FCGRT
DnaJ homolog subfamily C member 3	DNAJC3
C-type lectin domain family 11 member A	CLEC11A
DNA-3-methyladenine glycosylase	MPG
Nicotinate phosphoribosyltransferase	NAPRT
Torsin-1A	TOR1A
Protein disulfide-isomerase A5	PDIA5
Fibrillin-2	FBN2
Myeloblastin	PRTN3
Collagen alpha-1(VI) chain	COL6A1
Prostaglandin E synthase 2;Prostaglandin E synthase 2 truncated form	PTGES2
Cysteine-rich with EGF-like domain protein 2	CRELD2
Sulfhydryl oxidase 1	QSOX1
Aspartate aminotransferase, mitochondrial	GOT2
Mitochondrial amidoxime-reducing component 1	MARC1
Hypoxia up-regulated protein 1	HYOU1
OCIA domain-containing protein 1	OCIAD1
Protein transport protein Sec23B	SEC23B
GDP-fucose protein O-fucosyltransferase 1	POFUT1
CapZ-interacting protein	RCSD1
Liver carboxylesterase 1	CES1
Beta-hexosaminidase subunit beta	HEXB
Non-secretory ribonuclease	RNASE2
60S acidic ribosomal protein P2	RPLP2
Fumarate hydratase, mitochondrial	FH
Chitinase-3-like protein 1	CHI3L1
Carbonic anhydrase 2	CA2
Palmitoyl-protein thioesterase 1	PPT1
tRNA (guanine(26)-N(2))-dimethyltransferase	TRMT1
78 kDa glucose-regulated protein	HSPA5
Protein disulfide-isomerase A4	PDIA4
Syntenin-1	SDCBP
Endoplasmin	HSP90B1

Stimulation of shC cells with LPS for 4 h promoted substantial protein oxidation compared to unstimulated conditions. In total we identified 1061 proteins using mass spectrometry that became oxidized during LPS-stimulation (Table S1). Filtering for those proteins that reached the level of significance, LPS-stimulation oxidized 400 proteins compared to only 3 oxidatively modified proteins in the control group (Fig. 2B). Out of the 400 oxidized proteins 72 mitochondrial proteins were identified. Recapitulating the analysis in sh126B cells confirmed our assumption that a decrease in LPS-facilitated mtROS production resulted in less protein oxidation. In sh126B cells 40 proteins were significantly oxidized in response to LPS (Fig. 2C, Table S2). From these, only 3 mitochondrial proteins emerged. Taking into account that mtROS production in sh126B cells is impaired, implies a direct association between mtROS and mitochondrial protein oxidation. In a next step we directly compared proteins that became oxidized in either LPS-treated shC or sh126B cells, excluding those modified proteins that popped up in both samples (Table 1, Table S3).

With these filtering criteria we recognized 65 proteins after 4 h LPS-stimulation to be exclusively oxidized in shC cells. From these, 12 proteins are localized in mitochondria (labeled in yellow), with 2 of them being involved in oxidative phosphorylation (OXPHOS) (Fig. 2D). In sh126B cells, only 52 proteins were exclusively oxidized in response to LPS, among them only 2 mitochondrial proteins. These results underscore TMEM126B knockdown cells as a suitable model to analyze mtROS-dependent protein oxidation. We then concentrated on proteins within OXPHOS complexes that got oxidized upon LPS-addition (Fig. 2E). With this restriction an overall number of 18 proteins were identified. Without reaching significant values, NDUFA8 and NDUFA11 were identified to be oxidized in sh126B cells. In contrast, 16 proteins were recognized in shC cells, including several complex I members (NDUFB10, NDUFS1, NDUFB7, NDUFV1, NDUFA5, and NDUFB10). In addition, UQCRC2, UQCRC1, and UQCRFS1 of complex III, COX6C and COX4L1 of complex IV, and ATP5A1, ATP5O, ATP5J2, and ATP5H of complex V were detected. ATP5A1 was significantly oxidized upon LPS treatment in shC controls. Interestingly, ATP synthase was previously identified as a target of oxidative modifications [41]. Exposure of cells to H_2O_2 decreased the activity of complex V, which points to the redox-sensitivity of this complex [42]. Furthermore, ATP synthase activity was decreased by S-glutathionylation of ATP5A1 during oxidative stress in rat brain and liver [43]. A decreased ATP synthase activity by S-nitrosation of ATP5A1 was also reported to be protective for mouse hearts during myocardial ischemia [44]. Besides ATP5A1, succinate dehydrogenase flavoprotein subunit A (SDHA) was significantly oxidized in shC cells. SDHA was previously identified by gel-based stable isotope labeling of oxidized cysteines, aimed at detecting oxidized proteins in rat heart mitochondria after ischemia reperfusion [45]. Additionally, SDHA was found in a mass spectrometry approach with isotope-coded affinity tags of mouse hearts after ischemia/ reperfusion [46]. The protein also emerged in a screen, which identified mtROS formation at distinct sites of the respiratory chain coupled to the identification of respiratory complex specific protein oxidation patterns [11]. The authors identified SDHA to be oxidized by complex I ROS. This supports our hypothesis that complex I ROS are induced by LPS to cause protein oxidation. Considering that SDH was also reported to affect TLR4-signaling by inducing IL-1β via an increase of succinate makes this protein an ideal candidate for further studies [18,47].

3.4. Validation of SDHA

To validate SDHA as a target of LPS-induced mtROS, cells were treated with LPS, followed by a BIAM switch assay coupled with Western analysis (Fig. 3A and B).

In shC cells SDHA was partially oxidized even under basal conditions and oxidation became more pronounced after LPS addition. In sh126B cells LPS failed to increase SDHA oxidation. To prove the involvement of mtROS in SDHA oxidation, THP-1 cells were treated with

LPS in the presence and absence of mitoTEMPO (TEMPO) (Fig. 3C and D). Oxidation of SDHA by LPS was significantly blocked by TEMPO. In contrast, rotenone stimulated mtROS formation and enhanced SDHA oxidation, supporting the notion that complex I ROS cause SDHA oxidation. Fig. S2E shows a dose-dependent effect of rotenone on mtROS formation (Fig. S2E). In the following experiment we explored how SDHA oxidation affects SDH activity (Fig. 3E). LPS stimulation of shC cells significantly decreased SDH activity but enzyme inactivation was fully reversed by the addition of TEMPO. In sh126B cells basal SDH activity was slightly lower compared to shC cells, possibly due to marginally reduced protein expression (Fig. 3A). Importantly, SDH activity in sh126B cells was neither affected by LPS nor by TEMPO. Conclusively, mtROS oxidize SDHA and thereby decrease its activity in LPS-stimulated THP-1 cells, an effect requiring intact complex I.

Accumulation of succinate is known to occur in LPS-stimulated macrophages [18]. Glutamine-dependent anaplerosis and the GABA (γ-aminobutyric acid) shunt emerged as principle sources of its accumulation. However, why an intermediate of the TCA-cycle accumulates remained unclear from this work especially as succinate oxidation via SDH and an elevated mitochondrial membrane potential combine to drive mtROS production in LPS-stimulated macrophages [47]. One explanation towards succinate accumulation came from observations that itaconate, one of the most highly induced metabolites in classically activated macrophages, interferes with SDH activity [48]. These studies highlight succinate accumulation and/or metabolism as a critical mechanism controlling the macrophage proinflammatory state.

3.5. SDH inhibition induces HIF-1α

To link reduced SDH activity and TLR4 signaling, we inhibited SDH with atpenin A5 (AA5), which markedly reduced SDH activity (Fig. 4A).

A direct consequence of impaired SDH activity is the accumulation of succinate, an established PHD inhibitor. TCA-intermediates were shown to play a pivotal role in regulation of PHD activity. Besides α-ketoglutarate, which serves as cofactor, succinate and fumarate were identified as PHD inhibitors [49]. In cells lacking SDH or fumarate hydratase, succinate or fumarate accumulated, along with a reduced PHD activity and HIF-1α stabilization. PHD activity was restored by adding α-ketoglutarate derivatives, which competed with the inhibiting metabolites [50]. Since SDH activity was reduced by oxidation after LPS-treatment in our experiments, accumulation of the PHD-inhibitor succinate must be expected [18]. Thus, Western analysis of HIF-1α in AA5-treated cells were performed and showed a time-dependent accumulation of HIF-1α, starting at 1 h and reaching significant values after 2–4 h (Fig. 4B and C). The results support the notion that inhibition of SDH stabilizes HIF-1α. These findings open the possibility that ROS do not directly inhibit PHD activity to stabilize HIF-1α but act via SDH-inactivation and accumulation of TCA-cycle-intermediates. Previously, ROS formation has been linked to a decrease in the cellular anti-oxidative capacity and a limited availability of reduced iron (FeII) [51], with the notion that oxidized iron (FeIII) limits PHD activity [52]. Obviously, regulation of PHD activity is sensitive to a dysregulated cellular redox and/or metabolic homeostasis. To verify HIF-stabilization by succinate, cells were then treated with dimethyl succinate (DMS). Western analysis confirmed stabilization of HIF-1α in DMS-treated cells (Fig. 4D and E). Functionality of HIF-stabilization after SDH inhibition was proven by target gene expression profiles. Indeed, inhibition of SDH by AA5 caused mRNA expression of the HIF target genes Glut1, BNIP3, and IL-1β (Fig. 4 F-H). IL-1β appeared of special interest due to its role in inflammation and as an established cytokine induced by LPS.

3.6. IL-1β expression increased, while SDH activity decreased

To substantiate that AA5 induces IL-1β via HIF-1α, we analyzed mRNA expression of IL-1β in HIF-1α knockdown cells (sh1) exposed to
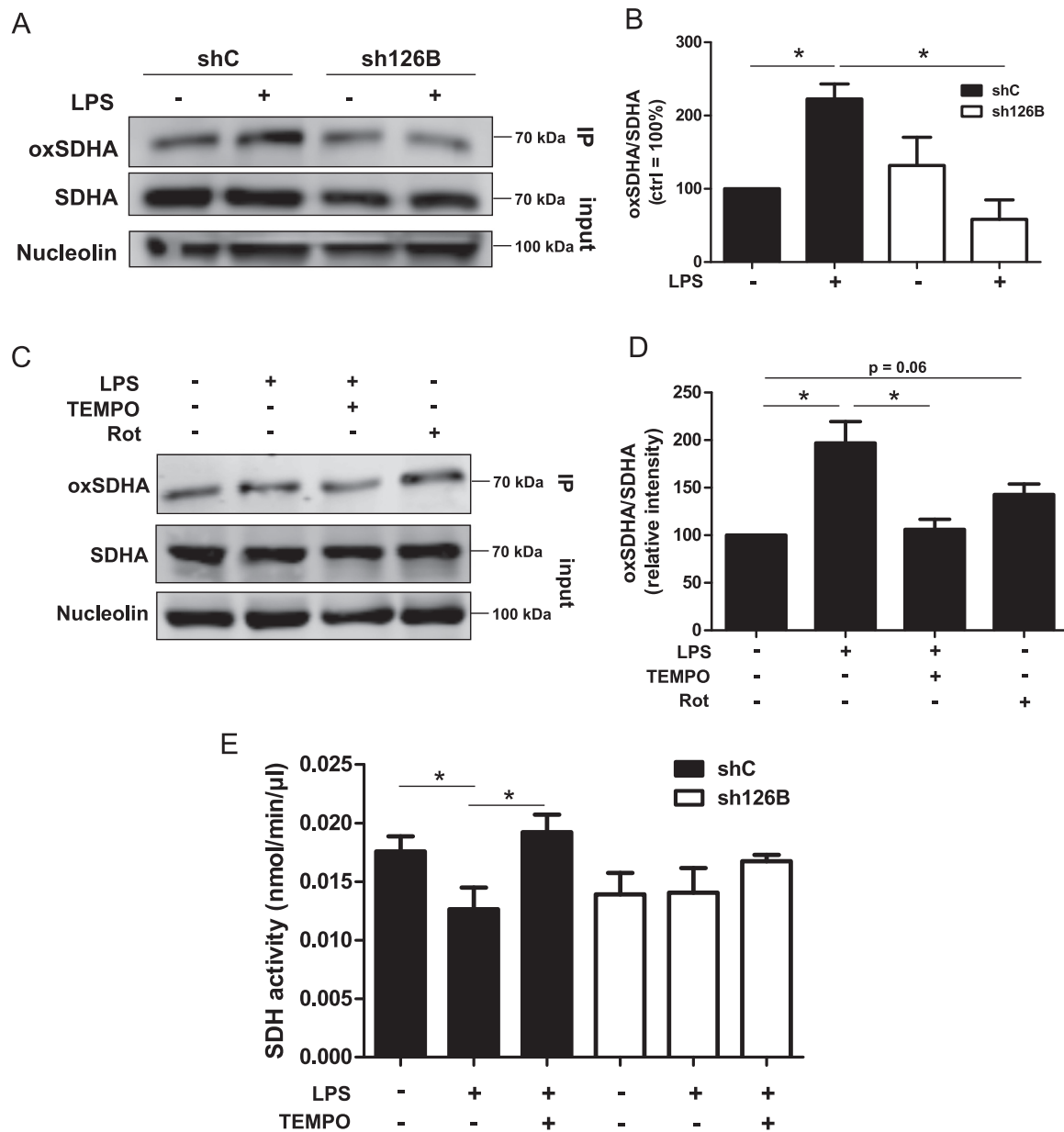
Fig. 3. Oxidation of succinate dehydrogenase. A. Control (shC) and TMEM126B knockdown (sh126B) THP-1 cells were treated with LPS for 4 h. Oxidized proteins were affinity purified using BIAM-switch assay followed by Western analysis of SDHA and nucleolin. B. Quantification of A. (n = 6). C. THP-1 cells were treated for 4 h with LPS, LPS and TEMPO, or rotenone (Rot) followed by the BIAM-switch assay and Western analysis for SDHA and nucleolin. D. Quantification of C (n = 7). E. SDH activity assay of shC and sh126B cells treated with either LPS or LPS plus TEMPO (n = 9). All data are mean values ± SEM, *p < 0.05.

AA5 (Fig. 4I, for validation of the HIF-1α knockdown see Fig. S2F). As expected, the IL-1β increase seen in control cells was absent in sh1 cells. We thereby confirmed previous studies, which established succinate as an inflammatory mediator, acting via HIF-1α [18]. Time-dependent accumulation of IL-1β mRNA after AA5-treatment started after 2 h and reached significance at 4 h (Fig. S3A). Temporally, this nicely overlaps with HIF-1α protein stabilization, which starts 1 h after AA5-treatment. The dose-response of IL-1β accumulation in response to AA5 is presented in Fig. S3B. AA5 elicited small effects at 100 nM and caused significant IL-1β mRNA expression at 1 µM. We then used TEMPO to prove that IL-1β mRNA expression demanded mtROS (Fig. 4J). After LPS-treatment, IL-1β mRNA increased, while the addition of TEMPO successfully prevented this rise. Previous studies showed that dimerization of the complex I assembly factor ECSIT with TNF receptor-associated factor 6 was needed to increase mtROS and cytokine production, thereby linking complex I to TLR4 signaling [14]. This

corroborates our findings, showing LPS-mediated IL-1β mRNA induction via HIF-1 and mtROS.

3.7. HIF-1α-stabilization in response to LPS-treatment

We now tested whether SDH inactivation in response to LPS-treatment stabilizes HIF-1α. There was a HIF-1α mRNA increase 1 h after LPS-addition with a maximum after 8 h and a slight decline towards 16 h incubations (Fig. 4K). Western analysis confirmed a time-dependent HIF-1α stabilization following LPS-treatment (Fig. 4L and M). Protein abundance started to increase after 4 h and continued to increase towards 8 and 16 h incubations. An early and rapid activation of NF-κB after LPS-addition is known and may account for the initial increase in HIF-1α mRNA expression [53]. Our experiments with rotenone and TMEM126B knockdown cells indicate that complex I ROS add to LPS-mediated HIF-1α stabilization. This implies a flexible system,
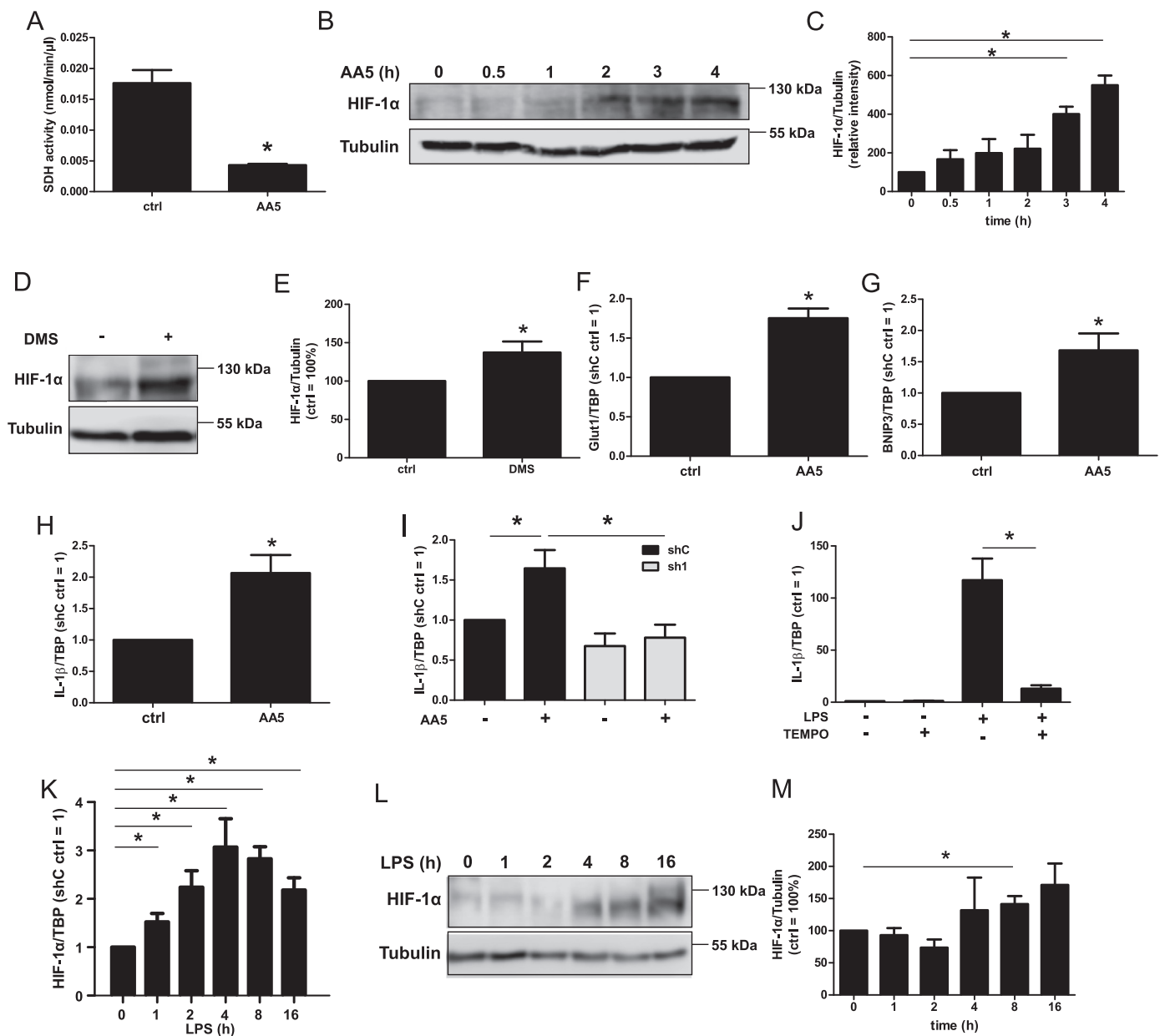
Fig. 4. HIF-1α induction after SDH inhibition. A. Succinate dehydrogenase (SDH) activity assay in THP-1 cells treated with the SDH inhibitor atpenin A5 (AA5). B. Time-dependent Western analysis of hypoxia inducible factor (HIF)-1α and tubulin in AA5-treated cells. C. Quantification of B (n = 4). D. THP-1 cells incubated for 6 h with dimethyl succinate (DMS) followed by Western analysis of HIF-1α and tubulin. E. Quantification of D (n = 5). F-H. mRNA expression of glucose transporter 1 (Glut1, F), CL2/adenovirus E1B 19 kDa protein-interacting protein 3 (BNIP3, G), and interleukin-1β (IL-1β, H) normalized to the TATA Box binding protein (TBP) after AA5-treatment (4 h) (n = 7). I. IL-1β mRNA analysis of AA5-treated control (shC, black bars) and HIF-1α knockdown (sh1, grey bars) cells (n = 4). J. THP-1 cells were incubated with LPS and TEMPO followed by IL-1β mRNA detection (n = 5). K. THP-1 cells were time-dependently treated with LPS followed by HIF-1α mRNA analysis (n = 7). L. Cells were time-dependently treated with LPS, followed by Western analysis of HIF-1α and tubulin. M. Quantification of L (n = 5). Data are mean values ± SEM, *p < 0.05.

where multiple sources of ROS contribute to HIF stabilization under normoxia, possibly via diverse signal transducing properties. ROS show an impact on HIF-1α regulation by either promoting its degradation or changing its transcription. [54]. Although regulation of HIF-1 by mtROS is versatile, oxidation of SDH and an increase in succinate points to a global metabolic rewiring to support inflammatory effector functions of macrophages.

3.8. IL-1β expression is reduced in sh126B cells

If a reduced SDH activity by oxidation enhances HIF-stabilization and IL-1β mRNA production, one would expect a decreased IL-1β

expression in sh126B cells after LPS-treatment because of impaired mtROS formation. Since, SDH activity was slightly decreased in sh126B cells, we ensured, that HIF-1α was not significantly stabilized under basal conditions in those cells (Fig. S3C and D). Next, we elucidated IL-1β expression in shC and sh126B cells, time-dependently stimulated with LPS (Fig. 5 A).

In shC cells IL-1β mRNA started to increase after 1 h, peaked after 2 h, and remained at moderate/high levels between 4 and 16 h. In sh126B cells the initial IL-1β mRNA increase was comparable but thereafter mRNA levels rapidly declined between 4 and 16 h with only a minor increase at 16 h compared to unstimulated controls. The initial increase with a peak of mRNA expression at 2 h is identical in shC and
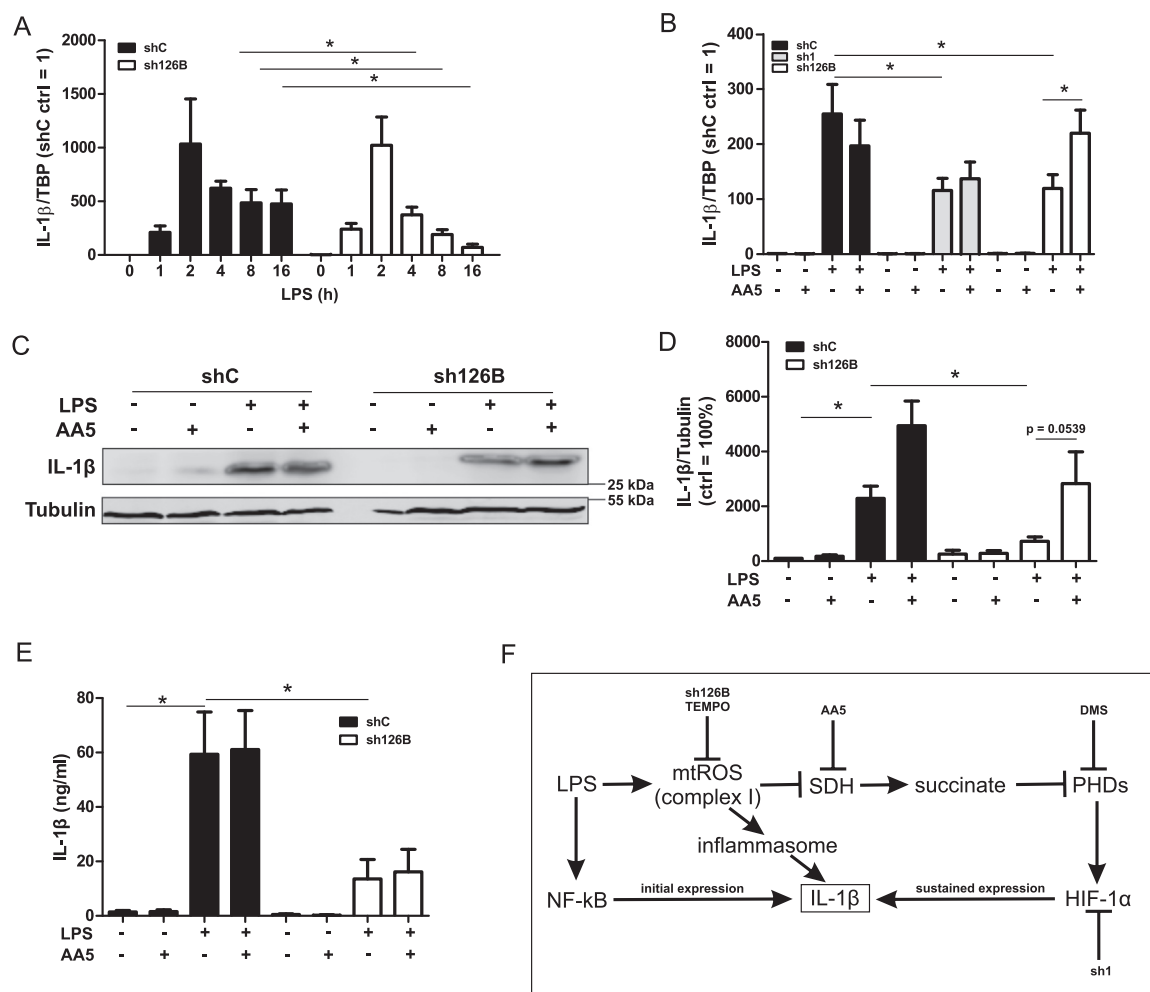
Fig. 5. IL-β expression in TMEM126B knockdown cells. A. Interleukin-1β (IL-1β) mRNA analysis in control (shC, black bars) and TMEM126B knockdown cells (sh126B, white bars) treated with LPS for indicated times (n = 7). B. shC, HIF-1α knockdown (sh1, grey bars), and sh126B cells were treated with LPS for 8 h, while atpenin A5 (AA5) was added for the last 4 h. IL-1β mRNA was analyzed (n = 7). C. Western analysis of IL-1β and tubulin in shC and sh126B cells treated with LPS for 8 h. AA5 was added for the last 4 h. D. Quantification of C (n = 7). E. Quantification of cytometric bead array for IL-1β in supernatants from experiments described in C (n = 5). F. Scheme of the proposed two-staged mechanism of IL-1β expression. Data are mean values ± SEM, *p < 0.05.

sh126B cells. We assume that this increase is NF-κB driven, especially as NF-κB activation, based on Western analysis of the phosphorylated NF-κB subunit p65, was comparable in wild type and TMEM125B knockout clones (Fig. S3E and F). Although ROS are reported to activate NF-κB, mitochondrial ROS are explicitly excluded to do so [55]. Time kinetics raised the question, whether HIF-1α accounts for sustained IL-1β mRNA expression in shC cells. Experimentally, shC, sh1, and sh126B cells were incubated for 8 h with LPS. After 4 h AA5 was added to mimic ROS-induced SDH inactivation, subsequent HIF-1α stabilization, followed by IL-1β mRNA expression (Fig. 5B). We noticed a profound IL-1β mRNA increase in control cells, which was unaltered by AA5, possibly because SDH already is inhibited/oxidized. In sh1 cells the response to LPS was significantly reduced, pointing to the requirement of HIF-1 in enhancing IL-1β mRNA expression, while the addition of AA5 had no effect in sh1 cells. Compared to shC, LPS-induced IL-1β expression in sh126B cells was decreased to the same extent as seen in sh1 cells. However, in these cells AA5 restored IL-1β expression nearly to control levels. Likely, this is facilitated by stabilization of HIF-1α by succinate, which of course was not possible in sh1 cells due to its knockdown. To also follow IL-1β expression at protein level, Western analyses were performed (Fig. 5C and D). Cells treated with AA5 showed a slight increase of IL-1β protein, while LPS-stimulation provoked a substantial and significant elevation in shC cells. In LPS-treated sh126B cells IL-1β increased to a lower degree compared to shC cells, corroborating mRNA

data. To test whether SDH inhibition augments IL-1β expression in sh126B cells as seen for mRNA expression, cells were treated with LPS plus AA5, which indeed led to IL-1β expression comparable to LPS-treated shC cells. Since IL-1β is processed by the inflammasome to its mature form, we used CBA-measurements to detect secreted and thus cleaved/active IL-1β (Fig. 5E). While control cells and AA5-treated macrophages did not facilitate IL-1β secretion, LPS stimulated shC cells released substantial amounts of IL-1β, which remained unaffected by AA5. sh126B cells release marginal amounts of IL-1β following LPS-stimulation, which were not increased by AA5. This appears rational, as for the secretion of IL-1β the immature, full-length version needs to be cleaved by the inflammasome and mtROS are known to trigger its assembly [56]. Therefore, reduced mtROS in sh126B cells may prohibit inflammasome activation and explain why IL-1β mRNA and protein expression are affected by AA5 but not its full maturation/secretion.

The link between succinate accumulation and HIF-1α stabilization, acting as a regulator of proinflammatory cytokine production in LPS-activated macrophages, is formally proven in several studies. Seminal investigations into the LPS – succinate - HIF-1α axis were undertaken by Tannahill and coworkers [18]. They noticed increased succinate levels in LPS-stimulated macrophages by the dominance of glutamine-dependent anerplerosis of the TCA-cycle leaving the question open why succinate accumulates albeit its further metabolism was not restricted. Lampropoulou and coworkers later on identified increased levels of

itaconate in LPS-stimulated macrophages and showed that this metabolite inhibits SDH and thereby increases succinate [48]. However, despite reduced SDH activity itaconate limited IL-1β formation. Moreover, in *IrG1* knockout cells, not being able to produce itaconate, succinate was low but HIF-1α mRNA and protein expression were increased, arguing against a simple and direct link between succinate levels and HIF-1-mediated proinflammatroy macrophage activation. Interestingly, Mills and coworkers identified itaconate as an inhibitor of Keap1. Inhibition of Keap1 activated Nrf2 activity, which promoted an anti-inflammatory phenotype by decreasing both HIF-1α and IL-1β [57]. These studies indicate a role of itaconate in anti-inflammatory signaling, which appears to limit pro-inflammatory events driven by succinate [58]. It was then realized that besides inhibition of PHD activity by succinate its oxidation by SDH is equally important to facilitate a pro-inflammatory response in LPS-activated macrophages [18]. This assumption is very well supported by our own data. We provide evidence that partial oxidation of SDH in LPS-stimulated macrophages lowers but not abrogates SDH activity. The accumulation of succinate appears substantial to block PHD activity, which in turn provokes HIF-1α stabilization and concomitant HIF-1 target gene activation. This includes IL-1β mRNA and protein expression, consistent with the notion that HIF-1 directly binds to a conserved hypoxia response element (HRE)-binding site in the promoter region of the *IL-1β* gene. As partial SDH oxidation still allows residual SDH activity the overall macrophage phenotype is shifted towards classical cell activation. Oxidation of SDH by mtROS must be considered a reversible process, highlighting how redox-signaling serves as a key regulatory node linking energy metabolism and inflammation. Our data point to complex I ROS as being critical for HIF-1α stabilization and highlights the role of the TCA-cycle intermediate succinate as the underlying signaling principle. Following TLR-4 activation, early NF-κB activation may triggers the initial IL-1β response, while the HIF-1 supporting pathway sustains IL-1β production at later times (Fig. 5F). Our study may also add to the controversy of mtROS in affecting HIF-1α, showing a modulating effect that is transmitted via protein oxidation. Further studies are needed to explore whether patients with complex I deficiency (e.g. Leigh syndrome) develop an altered inflammatory response to bacterial infections, which may result from reduced mtROS and an attenuated IL-1β response [59–61].

Acknowledgments

Funding

Appendix A. Supplementary material

Supplementary data associated with this article can be found in the online version at doi:10.1016/j.redox.2018.10.007.

References

[1] H. Heide, L. Bleier, M. Steger, J. Ackermann, S. Drose, B. Schwamb, M. Zornig, A.S. Reichert, I. Koch, I. Wittig, U. Brandt, Complexome profiling identifies TMEM126B as a component of the mitochondrial complex I assembly complex, Cell Metab. 16 (4) (2012) 538–549.

[2] R.O. Vogel, R.J.R.J. Janssen, M.A.M. van den Brand, C.E.J. Dieteren, S. Verkaart, W.J.H. Koopman, P.H.G.M. Willems, W. Pluk, L.P.W.J. van den Heuvel, J.A.M. Smeitink, L.G.J. Nijtmans, Cytosolic signaling protein Ecsit also localizes to mitochondria where it interacts with chaperone NDUFAF1 and functions in complex I assembly, Genes Dev. 21 (5) (2007) 615–624.

[3] B. Andrews, J. Carroll, S. Ding, I.M. Fearnley, J.E. Walker, Assembly factors for the membrane arm of human complex I, Proc. Natl. Acad. Sci. USA 110 (47) (2013) 18934–18939.

[4] S. Guerrero-Castillo, F. Baertling, D. Kownatzki, H.J. Wessels, S. Arnold, U. Brandt, L. Nijtmans, The assembly pathway of mitochondrial respiratory chain complex I, Cell Metab. 25 (1) (2017) 128–139.

[5] C. Wirth, U. Brandt, C. Hunte, V. Zickermann, Structure and function of mitochondrial complex I, Biochim. Biophys. Acta (2016).

[6] L. Sánchez-Caballero, B. Ruzzenente, L. Bianchi, Z. Assouline, G. Barcia, M.D. Metodiev, M. Rio, B. Funalot, M.A.M. van den Brand, S. Guerrero-Castillo, J.P. Molenaar, D. Koolen, U. Brandt, R.J. Rodenburg, L.G. Nijtmans, A. Rötig, Mutations in complex I assembly factor TMEM126B result in muscle weakness and isolated complex I deficiency, Am. J. Hum. Genet. 99 (1) (2016) 208–216.

[7] C.L. Alston, A.G. Compton, L.E. Formosa, V. Strecker, M. Oláhová, T.B. Haack, J. Smet, K. Stouffs, P. Diakumis, E. Ciara, D. Cassiman, N. Romain, J.W. Yarham, L. He, B. de Paepe, A.V. Vanlander, S. Seneca, R.G. Feichtinger, R. Płoski, D. Rokicki, E. Pronicka, R.G. Haller, J.L.K. van Hove, M. Bahlo, J.A. Mayr, R. van Coster, H. Prokisch, I. Wittig, M.T. Ryan, D.R. Thorburn, R.W. Taylor, Biallelic mutations in TMEM126B cause severe complex I deficiency with a variable clinical phenotype, Am. J. Hum. Genet. 99 (1) (2016) 217–227.

[8] D.C. Fuhrmann, I. Wittig, S. Dröse, T. Schmid, N. Dehne, B. Brüne, Degradation of the mitochondrial complex I assembly factor TMEM126B under chronic hypoxia, Cell. Mol. Life Sci. CMLS (2018).

[9] D.C. Fuhrmann, B. Brune, Mitochondrial composition and function under the control of hypoxia, Redox Biol. 12 (2017) 208–215.

[10] S. Drose, Differential effects of complex II on mitochondrial ROS production and their relation to cardioprotective pre- and postconditioning, Biochim. Biophys. Acta 1827 (5) (2013) 578–587.

[11] L. Bleier, I. Wittig, H. Heide, M. Steger, U. Brandt, S. Drose, Generator-specific targets of mitochondrial reactive oxygen species, Free Radic. Biol. Med. 78 (2015) 1–10.

[12] A. Weigert, A. von Knethen, D. Fuhrmann, N. Dehne, B. Brüne, Redox-signals and macrophage biology (for the upcoming issue of molecular aspects of medicine on signaling by reactive oxygen species), Mol. Asp. Med. (2018).

[13] S.M. Wi, G. Moon, J. Kim, S.-T. Kim, J.-H. Shim, E. Chun, K.-Y. Lee, TAK1-ECSIT-TRAF6 complex plays a key role in the TLR4 signal to activate NF-κB, J. Biol. Chem. 289 (51) (2014) 35205–35214.

[14] Y. Min, S.M. Wi, D. Shin, E. Chun, K.-Y. Lee, Peroxiredoxin-6 negatively regulates bactericidal activity and NF-κB activity by interrupting TRAF6-ECSIT complex, Front. Cell. Infect. Microbiol. 7 (2017) 94.

[15] T. Cramer, Y. Yamanishi, B.E. Clausen, I. Forster, R. Pawlinski, N. Mackman, V.H. Haase, R. Jaenisch, M. Corr, V. Nizet, G.S. Firestein, H.P. Gerber, N. Ferrara, R.S. Johnson, HIF-1alpha is essential for myeloid cell-mediated inflammation, Cell 112 (5) (2003) 645–657.

[16] X. Meng, B. Grötsch, Y. Luo, K.X. Knaup, M.S. Wiesener, X.-X. Chen, J. Jantsch, S. Fillatreau, G. Schett, A. Bozec, Hypoxia-inducible factor-1α is a critical transcription factor for IL-10-producing B cells in autoimmune disease, Nat. Commun. 9 (1) (2018) 251.

[17] M. Zhao, Y. Liu, R. Liu, J. Qi, Y. Hou, J. Chang, L. Ren, Upregulation of IL-11, an IL-6 family cytokine, promotes tumor progression and correlates with poor prognosis in non-small cell lung cancer, Cell. Phys. Biochem. Int. J. Exp. Cell. Physiol. Biochem. Pharmacol. 45 (6) (2018) 2213–2224.

[18] G.M. Tannahill, A.M. Curtis, J. Adamik, E.M. Palsson-McDermott, A.F. McGettrick, G. Goel, C. Frezza, N.J. Bernard, B. Kelly, N.H. Foley, L. Zheng, A. Gardet, Z. Tong, S.S. Jany, S.C. Corr, M. Haneklaus, B.E. Caffrey, K. Pierce, S. Walmsley, F.C. Beasley, E. Cummins, V. Nizet, M. Whyte, C.T. Taylor, H. Lin, S.L. Masters, E. Gottlieb, V.P. Kelly, C. Clish, P.E. Auron, R.J. Xavier, L.A.J. O'Neill, Succinate is an inflammatory signal that induces IL-1β through HIF-1α, Nature 496 (7444) (2013) 238–242.

[19] A.R. Sartori-Cintra, C.S. Mara, D.L. Argolo, I.B. Coimbra, Regulation of hypoxia-inducible factor-1alpha (HIF-1alpha) expression by interleukin-1beta (IL-1 beta), insulin-like growth factors I (IGF-I) and II (IGF-II) in human osteoarthritic chondrocytes, Clinics 67 (1) (2012) 35–40.

[20] N. Dehne, D. Fuhrmann, B. Brune, Hypoxia-inducible factor (HIF) in hormone signaling during health and disease, Cardiovasc. Hematol. Agents Med. Chem. 11 (2) (2013) 125–135.

[21] J.J. Briere, J. Favier, P. Benit, V. El Ghouzzi, A. Lorenzato, D. Rabier, M.F. Di Renzo, A.P. Gimenez-Roqueplo, P. Rustin, Mitochondrial succinate is instrumental for HIF1alpha nuclear translocation in SDHA-mutant fibroblasts under normoxic conditions, Hum. Mol. Genet. 14 (21) (2005) 3263–3269.

[22] T. Klimova, N.S. Chandel, Mitochondrial complex III regulates hypoxic activation of HIF, Cell Death Differ. 15 (4) (2008) 660–666.

[23] M.A. Selak, S.M. Armour, E.D. MacKenzie, H. Boulahbel, D.G. Watson, K.D. Mansfield, Y. Pan, M.C. Simon, C.B. Thompson, E. Gottlieb, Succinate links TCA cycle dysfunction to oncogenesis by inhibiting HIF-alpha prolyl hydroxylase, Cancer Cell 7 (1) (2005) 77–85.

[24] N.S. Chandel, D.S. McClintock, C.E. Feliciano, T.M. Wood, J.A. Melendez, A.M. Rodriguez, P.T. Schumacker, Reactive oxygen species generated at mitochondrial complex III stabilize hypoxia-inducible factor-1alpha during hypoxia: a mechanism of O2 sensing, J. Biol. Chem. 275 (33) (2000) 25130–25138.

[25] Y. Guo, B. Han, K. Luo, Z. Ren, L. Cai, L. Sun, NOX2-ROS-HIF-1α signaling is critical for the inhibitory effect of oleanolic acid on rectal cancer cell proliferation, Biomed. Pharmacother. = Biomed. Pharmacother. 85 (2017) 733–739.

[26] G. Comito, M. Calvani, E. Giannoni, F. Bianchini, L. Calorini, E. Torre, C. Migliore, S. Giordano, P. Chiarugi, HIF-1alpha stabilization by mitochondrial ROS promotes

Met-dependent invasive growth and vasculogenic mimicry in melanoma cells, Free Radic. Biol. Med. 51 (4) (2011) 893–904.

[27] E.C. Vaux, E. Metzen, K.M. Yeates, P.J. Ratcliffe, Regulation of hypoxia-inducible factor is preserved in the absence of a functioning mitochondrial respiratory chain, Blood 98 (2) (2001) 296–302.

[28] N. Masson, P.J. Ratcliffe, Hypoxia signaling pathways in cancer metabolism: the importance of co-selecting interconnected physiological pathways, Cancer Metab. 2 (1) (2014) 3.

[29] K. Nishi, T. Oda, S. Takabuchi, S. Oda, K. Fukuda, T. Adachi, G.L. Semenza, K. Shingu, K. Hirota, LPS induces hypoxia-inducible factor 1 activation in macrophage-differentiated cells in a reactive oxygen species-dependent manner, Antioxid. Redox Signal 10 (5) (2008) 983–995.

[30] N.A. Kulak, G. Pichler, I. Paron, N. Nagaraj, M. Mann, Minimal, encapsulated proteomic-sample processing applied to copy-number estimation in eukaryotic cells, Nat. Methods 11 (3) (2014) 319–324.

[31] J.V. Olsen, L.M.F. de Godoy, G. Li, B. Macek, P. Mortensen, R. Pesch, A. Makarov, O. Lange, S. Horning, M. Mann, Parts per million mass accuracy on an Orbitrap mass spectrometer via lock mass injection into a C-trap, Mol. Cell. Proteom. MCP 4 (12) (2005) 2010–2021.

[32] S. Tyanova, T. Temu, P. Sinitcyn, A. Carlson, M.Y. Hein, T. Geiger, M. Mann, J. Cox, The Perseus computational platform for comprehensive analysis of (prote)omics data, Nat. Methods 13 (9) (2016) 731–740.

[33] J. Cox, M. Mann, MaxQuant enables high peptide identification rates, individualized p.p.b.-range mass accuracies and proteome-wide protein quantification, Nat. Biotechnol. 26 (12) (2008) 1367–1372.

[34] I. Wittig, H.P. Braun, H. Schagger, Blue native PAGE, Nat. Protoc. 1 (1) (2006) 418–428.

[35] J. Fan, J.J. Kamphorst, R. Mathew, M.K. Chung, E. White, T. Shlomi, J.D. Rabinowitz, Glutamine-driven oxidative phosphorylation is a major ATP source in transformed mammalian cells in both normoxia and hypoxia, Mol. Syst. Biol. 9 (2013) 712.

[36] D. Xiao, L. Zeng, K. Yao, X. Kong, G. Wu, Y. Yin, The glutamine-alpha-ketoglutarate (AKG) metabolism and its nutritional implications, Amino Acids 48 (9) (2016) 2067–2080.

[37] J. Pfleger, M. He, M. Abdellatif, Mitochondrial complex II is a source of the reserve respiratory capacity that is regulated by metabolic sensors and promotes cell survival, Cell Death Dis. 6 (2015) e1835.

[38] N.J. Watmough, F.E. Frerman, The electron transfer flavoprotein: ubiquinone oxidoreductases, Biochim. Biophys. Acta 1797 (12) (2010) 1910–1916.

[39] N. Imaizumi, K. Kwang Lee, C. Zhang, U.A. Boelsterli, Mechanisms of cell death pathway activation following drug-induced inhibition of mitochondrial complex I, Redox Biol. 4 (2015) 279–288.

[40] H.K. Fam, K. Choi, L. Fougner, C.J. Lim, C.F. Boerkoel, Reactive oxygen species stress increases accumulation of tyrosyl-DNA phsosphodiesterase 1 within mitochondria, Sci. Rep. 8 (1) (2018) 4304.

[41] N. Kaludercic, V. Giorgio, The dual function of reactive oxygen/nitrogen species in bioenergetics and cell death: the role of ATP synthase, Oxid. Med. Cell. Longev. 2016 (2016) 3869610.

[42] G. Lippe, M. Comelli, D. Mazziliss, F. Dabbeni Sal, I, Mavelli, The inactivation of mitochondrial F1 ATPase by H2O2 is mediated by iron ions not tightly bound in the protein, Biochem. Biophys. Res. Commun. 181 (2) (1991) 764–770.

[43] J. Garcia, D. Han, H. Sancheti, L.-P. Yap, N. Kaplowitz, E. Cadenas, Regulation of mitochondrial glutathione redox status and protein glutathionylation by respiratory substrates, J. Biol. Chem. 285 (51) (2010) 39646–39654.

[44] J. Sun, M. Morgan, R.-F. Shen, C. Steenbergen, E. Murphy, Preconditioning results in S-nitrosylation of proteins involved in regulation of mitochondrial energetics and calcium transport, Circ. Res. 101 (11) (2007) 1155–1163.

[45] P. Martínez-Acedo, E. Núñez, F.J.S. Gómez, M. Moreno, E. Ramos, A. Izquierdo-Álvarez, E. Miró-Casas, R. Mesa, P. Sánchez-Quiles, S. Calvo, C. Andrés-Lacueva, D.G. Dorado, S. Lamas, J. Vázquez, A novel strategy for global analysis of the dynamic thiol redox proteome, Mol. Cell. Proteom. MCP 11 (9) (2012) 800–813.

[46] V. Kumar, T. Kleffmann, M.B. Hampton, M.B. Cannell, C.C. Winterbourn, Redox proteomics of thiol proteins in mouse heart during ischemia/reperfusion using ICAT reagents and mass spectrometry, Free Radic. Biol. Med. 58 (2013) 109–117.

[47] E.L. Mills, B. Kelly, A. Logan, A.S.H. Costa, M. Varma, C.E. Bryant, P. Tourlomousis, J.H.M. Däbritz, E. Gottlieb, I. Latorre, S.C. Corr, G. McManus, D. Ryan, H.T. Jacobs, M. Szibor, R.J. Xavier, T. Braun, C. Frezza, M.P. Murphy, L.A. O'Neill, Succinate dehydrogenase supports metabolic repurposing of mitochondria to drive inflammatory macrophages, Cell 167 (2) (2016) 457–470 (e13).

[48] V. Lampropoulou, A. Sergushichev, M. Bambouskova, S. Nair, E.E. Vincent, E. Loginicheva, L. Cervantes-Barragan, X. Ma, S.C.-C. Huang, T. Griss, C.J. Weinheimer, S. Khader, G.J. Randolph, E.J. Pearce, R.G. Jones, A. Diwan, M.S. Diamond, M.N. Artyomov, Itaconate links inhibition of succinate dehydrogenase with macrophage metabolic remodeling and regulation of inflammation, Cell Metab. 24 (1) (2016) 158–166.

[49] A. King, M.A. Selak, E. Gottlieb, Succinate dehydrogenase and fumarate hydratase: linking mitochondrial dysfunction and cancer, Oncogene 25 (34) (2006) 4675–4682.

[50] E.D. MacKenzie, M.A. Selak, D.A. Tennant, L.J. Payne, S. Crosby, C.M. Frederiksen, D.G. Watson, E. Gottlieb, Cell-permeating alpha-ketoglutarate derivatives alleviate pseudohypoxia in succinate dehydrogenase-deficient cells, Mol. Cell. Biol. 27 (9) (2007) 3282–3289.

[51] D. Gerald, E. Berra, Y.M. Frapart, D.A. Chan, A.J. Giaccia, D. Mansuy, J. Pouysségur, M. Yaniv, F. Mechta-Grigoriou, JunD reduces tumor angiogenesis by protecting cells from oxidative stress, Cell 118 (6) (2004) 781–794.

[52] B.W. Wong, A. Kuchnio, U. Bruning, P. Carmeliet, Emerging novel functions of the oxygen-sensing prolyl hydroxylase domain enzymes, Trends Biochem. Sci. 38 (1) (2013) 3–11.

[53] S. Frede, C. Stockmann, P. Freitag, J. Fandrey, Bacterial lipopolysaccharide induces HIF-1 activation in human monocytes via p44/42 MAPK and NF-kappaB, Biochem. J. 396 (3) (2006) 517–527.

[54] A.N. Shvetsova, D. Mennerich, J.M. Kerätär, J.K. Hiltunen, T. Kietzmann, Non-electron transfer chain mitochondrial defects differently regulate HIF-1α degradation and transcription, Redox Biol. 12 (2017) 1052–1061.

[55] G. Gloire, S. Legrand-Poels, J. Piette, NF-kappaB activation by reactive oxygen species: fifteen years later, Biochem. Pharmacol. 72 (11) (2006) 1493–1505.

[56] P. Gan, Z. Gao, X. Zhao, G. Qi, Surfactin inducing mitochondria-dependent ROS to activate MAPKs, NF-κB and inflammasomes in macrophages for adjuvant activity, Sci. Rep. 6 (2016) 39303.

[57] E.L. Mills, D.G. Ryan, H.A. Prag, D. Dikovskaya, D. Menon, Z. Zaslona, M.P. Jedrychowski, A.S.H. Costa, M. Higgins, E. Hams, J. Szpyt, M.C. Runtsch, M.S. King, J.F. McGouran, R. Fischer, B.M. Kessler, A.F. McGettrick, M.M. Hughes, R.G. Carroll, L.M. Booty, E.V. Knatko, P.J. Meakin, M.L.J. Ashford, L.K. Modis, G. Brunori, D.C. Sévin, P.G. Fallon, S.T. Caldwell, E.R.S. Kunji, E.T. Chouchani, C. Frezza, A.T. Dinkova-Kostova, R.C. Hartley, M.P. Murphy, L.A. O'Neill, Itaconate is an anti-inflammatory metabolite that activates Nrf2 via alkylation of KEAP1, Nature 556 (7699) (2018) 113–117.

[58] M.P. Murphy, L.A.J. O'Neill, Krebs cycle reimagined: the emerging roles of succinate and itaconate as signal transducers, Cell 174 (4) (2018) 780–784.

[59] P. Benit, A. Slama, F. Cartault, I. Giurgea, D. Chretien, S. Lebon, C. Marsac, A. Munnich, A. Rotig, P. Rustin, Mutant NDUFS3 subunit of mitochondrial complex I causes Leigh syndrome, J. Med. Genet. 41 (1) (2004) 14–17.

[60] L.H. Ngu, L.G. Nijtmans, F. Distelmaier, H. Venselaar, S.E. van Emst-de Vries, M.A. van den Brand, B.J. Stoltenborg, L.T. Wintjes, P.H. Willems, L.P. van den Heuvel, J.A. Smeitink, R.J. Rodenburg, A catalytic defect in mitochondrial respiratory chain complex I due to a mutation in NDUFS2 in a patient with Leigh syndrome, Biochim. Biophys. Acta 1822 (2) (2012) 168–175.

[61] C. Ugalde, R. Hinttala, S. Timal, R. Smeets, R.J. Rodenburg, J. Uusimaa, L.P. van Heuvel, L.G. Nijtmans, K. Majamaa, J.A. Smeitink, Mutated ND2 impairs mitochondrial complex I assembly and leads to Leigh syndrome, Mol. Genet. Metab. 90 (1) (2007) 10–14.